REPORT DOCUMENTATION PAGE

1

Form Approved OMB NO. 0704-0188

1. REPORT DATE (DD-MM-YYYY)	2. REPORT TYPE	3. DATES COVERED (From - To)
29-08-2014	Book Chapter	-

4. TITLE AND SUBTITLE
Nanosensors based on DNA and RNA Aptamers, and Semiconductor Quantum Dots

5a. CONTRACT NUMBER
W911NF-11-1-0024

5b. GRANT NUMBER

5c. PROGRAM ELEMENT NUMBER
611103

6. AUTHORS
Shipryia Poduri, Ke Xu, Xenia Meshik, Saddia M. Ranginwala, Pitamber Shukla, Nanzhu Zhang, Mitra Dutta, Michael A. Stroscio, Jun Qian, TsaiChin Wu, Kimber Brenneman, Banani Sen

5d. PROJECT NUMBER

5e. TASK NUMBER

5f. WORK UNIT NUMBER

7. PERFORMING ORGANIZATION NAMES AND ADDRESSES
University of California - Irvine
5171 California Ave., Suite 150

Irvine, CA 92697 -7600

8. PERFORMING ORGANIZATION REPORT NUMBER

9. SPONSORING/MONITORING AGENCY NAME(S) AND ADDRESS (ES)
U.S. Army Research Office
P.O. Box 12211
Research Triangle Park, NC 27709-2211

10. SPONSOR/MONITOR'S ACRONYM(S)
ARO

11. SPONSOR/MONITOR'S REPORT NUMBER(S)
58162-EL-MUR.76

12. DISTRIBUTION AVAILIBILITY STATEMENT
Approved for public release; distribution is unlimited.

13. SUPPLEMENTARY NOTES
The views, opinions and/or findings contained in this report are those of the author(s) and should not contrued as an official Department of the Army position, policy or decision, unless so designated by other documentation.

14. ABSTRACT
see attached

15. SUBJECT TERMS
dna, nanotechnology

16. SECURITY CLASSIFICATION OF:			17. LIMITATION OF ABSTRACT	15. NUMBER OF PAGES	19a. NAME OF RESPONSIBLE PERSON
a. REPORT	b. ABSTRACT	c. THIS PAGE			Peter Burke
UU	UU	UU	UU		19b. TELEPHONE NUMBER 949-824-9326

Report Title

Nanosensors based on DNA and RNA Aptamers, and Semiconductor Quantum Dots

ABSTRACT

see attached

Nanosensors Based on DNA and RNA Aptamers and Semiconductor Quantum Dots

Mitra Dutta
ECE Department, University of Illinois at Chicago, Chicago, Illinois, U.S.A.
Physics Department, University of Illinois at Chicago, Chicago, Illinois, U.S.A.

Michael A. Stroscio
ECE Department, University of Illinois at Chicago, Chicago, Illinois, U.S.A.
Physics Department, University of Illinois at Chicago, Chicago, Illinois, U.S.A.
BioE Department, University of Illinois at Chicago, Chicago, Illinois, U.S.A.

Jun Qian
ECE Department, University of Illinois at Chicago, Chicago, Illinois, U.S.A.

TsaiChin Wu
ECE Department, University of Illinois at Chicago, Chicago, Illinois, U.S.A.
Physics Department, University of Illinois at Chicago, Chicago, Illinois, U.S.A.

Kimber Brenneman
BioE Department, University of Illinois at Chicago, Chicago, Illinois, U.S.A.

Banani Sen
ECE Department, University of Illinois at Chicago, Chicago, Illinois, U.S.A.

Shripriya Poduri
Ke Xu
Xenia Meshik
Saadia M. Ranginwala
Pitamber Shukla
BioE Department, University of Illinois at Chicago, Chicago, Illinois, U.S.A.

Nanzhu Zhang
ECE Department, University of Illinois at Chicago, Chicago, Illinois, U.S.A.

Abstract
In this entry, novel nanosensors based on the use of DNA and RNA molecules that selectively bind to analytes in combination with 1) nanoscale donor complexes or 2) semiconductor quantum dots are discussed. Of central importance in these novel nanosensors are DNA or RNA molecules that change their conformational state when they bind selectively to an analyte. This conformational change is exploited to produce an electrical signal from a nanoscale donor complex or an optical signature from a semiconductor quantum dot. Selected examples of such nanosensors are given for the cases of electrical and optical output signals.

INTRODUCTION

Nanosensors based on the use of DNA or RNA molecules that selectively bind to analytes and change their conformational shape are discussed for two separate cases: nanosensors based on 1) nanoscale donor complexes or 2) semiconductor quantum dots. Of central importance in these novel nanosensors are DNA or RNA molecules that change their conformational state when they bind selectively to an analyte. This conformational change is exploited to produce an electrical signal from a nanoscale donor complex or an optical signature from a semiconductor quantum dot.

Aptamers are artificial short DNA or RNA molecules that bind to analytes of interest including proteins,[1] cells,[2] DNA,[3] inorganic ions,[4] and small molecules[5–7] with high specificity. The science and technology of aptamers has advanced rapidly based on techniques that exploit combinatorial libraries of synthetic nucleic acids by a process of adsorption, recovery, and amplification known as systematic evolution of ligands by exponential enrichment (SELEX).[8] The selective binding of aptamers is

Dekker Encyclopedia of Nanoscience and Nanotechnology DOI: 10.1081/E-ENN2-120048425

similar to that of antibodies but aptamers enjoy a number of advantages:

1. Aptamers are more stable than antibodies for long-term storage without degradation and they can be used multiple times without loss of sensitivity.[9]
2. Aptamers may be prepared cost-effectively through automatic animal-free synthesis in vitro and they may be modified easily through additional engineering and chemistry to include end functional units for immobilization[10] or fluorophore capabilities.[7,11,12]
3. Aptamers are generally several dozen bases in length and are therefore smaller than antibodies.

In this discussion, the use of aptamers in combination with 1) nanoscale donor complexes for an electrical output signature and 2) semiconductor quantum dots for an optical output mode is discussed.

ELECTRICAL NANOSENSORS BASED ON APTAMERS AND NANOSCALE DONOR COMPLEXES

The use of aptamers for electrical detection of analytes is illustrated convincingly by the recent works on label-free electronic detection of thrombin in blood serum by using an aptamer-based sensor;[1] aptamer-based electrochemical detection of picomolar platelet-derived growth factor directly in blood serum;[2] label-free electrochemical detection of DNA in blood serum via target-induced resolution of an electrode-bound DNA pseudoknot;[3] aptamer-based small-molecule sensor for the rapid, label-free detection of cocaine in adulterated samples and biological fluids;[13] and high-specificity, electrochemical sandwich assays based on single aptamer sequences and suitable for the direct detection of small-molecule targets in blood and other complex matrices.[14]

In these studies, one of the detection modalities is based on binding one end of a DNA aptamer to a conducting substrate and functioning the free end of the aptamer with a molecule that acts as a charge donor when it comes in close proximity to the conducting substrate. In exploiting this detection modality, the aptamer is selected so that upon binding to the analyte, it changes its conformation so that the end functionalized with the charge donor moves close to the conducting substrate transfer its charge to the substrate or is immobilized on the surface of the conducting substrate. Thus, the aptamer-based detector is in the "off" state before the analyte is introduced and in the "on" charge transfer state that corresponds to the increase in the current in the conducting substrate. In each individual type of aptamer-based detector, it is necessary to select a DNA molecule that binds selectively to the analyte[5,7] and undergoes a conformational change that cause the detector to switch between the off and on states. Pioneering research on reversible aptamer-based molecular sensors has used a Au substrate as the conducting substrate for the sensor.[13]

These pioneering studies[13] have recently been extended to the case of single-step, label-free aptamer electrical sensors on a graphene field-effect transistor (FET) structure based on analyte binding-induced folding of the aptamer probe. In this example of an aptamer-based nanosensor with electrical output, a cocaine aptamer[5,7,13] is modified with methylene blue (MB) at the 3′ end and bound to the graphene-like surface of a micron-sized graphite structure having a thickness of roughly 10 layers of graphene, that is, a thickness of approximately a few nanometers. Before the introduction of the analyte (cocaine), this aptamer-based graphene FET device is in the off state, and after the introduction of the analyte, the sensor is in the on state since it is found to manifest a current for cocaine concentrations in the micromole concentration range. This nanosensor is an example of a biological–chemical sensor that converts a biological or chemical response into an electronic signal. Similar aptamer-based sensors have been discussed in the literature; examples are electrochemical sensors[1–4] and electrical sensors.[15–17] Indeed, aptamer-modified carbon nanotube (CNT) FETs[13,17] and Si nanowire[16] FET electrical sensors have been successfully fabricated. In the present example, a thin layer of graphite is used as the substrate since graphene has ultrahigh mobility and high surface-to-volume ratio and is very promising for an ultrasensitive label-free detection of molecules.[13,14]

Based on the previously successful detection of cocaine,[13] cocaine is chosen to be the analyte for testing the graphene FET aptamer sensor as shown in Fig. 1. The aptamer[5] modified with MB[13] was used to detect the cocaine binding through charge transport to the surface of the graphite upon the cocaine-induced conformational change of the DNA aptamer. MB is an electron donor with a LUMO level at –3.6 eV relative to vacuum and a HOMO level at –5.1 eV relative to vacuum; moreover, chemical oxidation–reduction-synthesized graphene[20] usually shows p-type semiconductor behavior with holes as carriers. Indeed, intrinsic graphene has a Dirac point at about

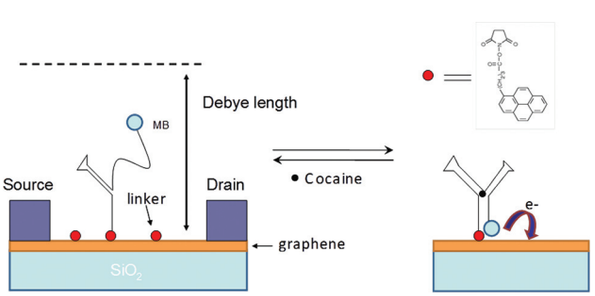

Fig. 1 Graphene-like FET aptamer sensor in off state and on state.

–4.0 eV relative to vacuum, but the presence of air or water usually lowers the Fermi level to about 2.0 eV below the Dirac point yield in a p-type material with a Fermi level below the LUMO and HOMO levels of MB. 1-Pyrenebutanoic acid, succinimidyl ester (designation is P130 in Fig. 1) as the red dot in Fig. 1, is used as linker molecule to non-covalently bind the aptamer to the graphene surface by the pyrene group as the protocol for CNTs.[10,21] The cocaine aptamer is about 30 bases long, or approximately 10 nm long; specifically, the functionalized cocaine aptamer is six-carbon amino at the 5′ end and seven-carbon MB modified at the 3′ end probe DNA as NH2-C6-5′-GAC AAG GAA AAT CCT TCA ATG AAG TGG GTC-3′-C7-MB. The Debye length,[17] which is defined as the typical distance required for screening the surplus charge by the mobile carrier present in a material,[22] may also be of this magnitude for electrolytes with appropriately chosen ions and ion concentrations. As discussed previously, when the analyte molecule, cocaine in this case, is present, the aptamer will undergo a conformation change and thus change the distance between the MB and the graphene surface, changing the electrical properties of the graphene FET.

In this example, a cocaine hydrochloride solution, 1.0 mg/mL ± 5% in methanol, was dissolved in Milli-Q water to desired concentration to be ready for testing as needed. In addition, phosphate-buffered saline (PBS) buffer solution is used (10 nM phosphate with 1.0 NaCl and 1 mM Mg^{2+}).

Graphene is synthesized by a chemical oxidation and reduction method.[20] First, graphite powder is oxidized by the general method;[23] then, the graphite oxide is reduced by the highly toxic hydrazine under N_2 atmosphere. A one-step liquid exfoliation method[24,25] is also used to synthesize multiple-layer graphene sheets. First, the graphite powder is ultrasonicated in *N*-methyl-2-pyrrolidinone for 1 hr. Then, the dispersion is left to stand for 24 hr, and it is centrifuged for 90 min at 1500 rpm. After centrifugation, the top solution is taken for future usage. These graphite structures are drop coated on a 300 nm thick SiO_2 film on a Si wafer and then carefully selected by optical microscopy and confirmed by Raman and atomic force microscopy measurements. The graphite structures are tens of micrometers in scale. In our device, multiple-layer graphene sheets are used for their sustainability to lithography process. Optical lithography is use to fabricate the source and drain electrodes on the multilayer graphene sheets. During the lithography process, the key point is to locate the multilayer graphene sheet under the MJB3 mask aligner, so an iron oxide transparent mask is used during our process. S1818 is used as the positive photoresist. A 50 nm thick electrode, consisting of a 45 nm Au layer and a 5 nm Cr contact layer, is deposited by electron beam evaporation. After Au deposition, the device is cleaned ultrasonically in acetone for 1 min to strip the photoresist. The aptamer functionalized with MB is bound to the multilayer graphene surface as follows: a 10 μL (adjustable according to the total wafer surface to cover the working area) variable-concentration (from 100 pM to 10 μM) cocaine aptamer solution is deposited on the graphene surface and incubated overnight at room temperature and at ~70% humidity. As a final step, the structure is rinsed with deionized water and blow dried in N_2. A Raman spectrometer is used to study the vibrational, rotational, and other low-frequency modes in a system. Indeed, Raman scattering has been widely used to identify the monolayer or multilayer graphene[26–30] and study the DNA vibrational modes.[31,32] Raman spectra of the devices with immobilized cocaine aptamer were acquired by a Renishaw micro-Raman apparatus with an Ar+ ion laser (514.5 nm wavelength) at a power level of 8 mW. The grating is set as 1800 gr/mm providing a resolution of 0.8 cm^{-1}. The Leica microscope has 50X, 20X, and 5X objective lenses as well as a CCD camera for viewing, and the laser beam is focused on the sample through a specialized microscope eyepiece (Olympus, 50X) down to a focal spot size of approximately 1 μm. The exact position of the sample is driven by a translation stage. The spectrum is collected as a point-to-point basis. The system has a depth resolution of about 2 μm and a spatial resolution of about 1 μm. The *I–V* characteristics of these aptamer-based FETs were studied with a HP 4156B semiconductor parameter analyzer. In the tests, the cocaine solution was dropped on the working area and left to dry for a few minutes, and then the source drain current is collected versus variable backgate voltage. To refresh the working area, the device is dipped in PBS buffer for 5 min after every test. Source drain current curves versus variable backgate voltage has been studied for the aptamer-based FET exposed to aptamer-immobilized, 1 μM, 10 μM, and 100 μM cocaine solutions. The I_{SD} curves illustrate typical p-type graphene behavior,[20,33] where the current decreases with increasing V_{BG} from -60 V to 60 V. After the cocaine aptamer immobilized on the graphene surface, the I_{SD} current still performs as a p-type semiconductor but experiences a current decrease from 20.5 μA to 15.8 μA at -60 V and from 19.7 μA to 15 μA. The current decrease amplitude of the whole V_{BG} scale is consistent for about 4.7 μA, which means that the current decrease caused by the attached aptamer is stable in the variable V_{BG}. Further, when cocaine is present, the I_{SD} continues to reduce with increasing concentration of cocaine. At -60 V, the current drops from 15.8 μA to 10.5 μA, 9.7 μA, and 9.4 μA, while at 60 V, the current drops from 15.0 μA to 10.0 μA, 9.2μA, and 9.0 μA. These results imply that the negative charge from the BM is lowering the effective p-type current in the device. The current decrease or conductance reduction is very close in the whole V_{BG} scale. From these results, the sensor works as a "signal-off" sensor when cocaine is present.

The graphite-based FET-like aptamer sensor for cocaine has been fabricated using combined semiconductor techniques and molecular biological protocols. This nanosensor is of the type discussed previously in Ref. 13. In the

present case, the signal-off sensor has shown sensitivity in the 1 to 100 μM range.

OPTICAL NANOSENSORS BASED ON APTAMERS AND SEMICONDUCTOR QUANTUM DOTS

The use of aptamers as the basis for nanosensors with electrical outputs is complemented by aptamer-based sensors that function on the basis of the modulation of an optical signal upon the analyte-induced change in conformation of the aptamer. These aptamer-based optical output sensors are in many cases configured with a nanoscale optical emitter—a dye or semiconductor quantum dot—on one end of the aptamer and a nanostructure that quenches the output of the dye or semiconductor quantum dot on the other end of the aptamer. For this type of nanosensor to function as an analyte detector, the aptamer must change its conformation when it binds to the analyte in a way that results in a change in the degree of quenching of the nanoscale optical emitter. The case of interest in the present discussion is the case where an emitting quantum dot bound to one end of the aptamer experiences an analyte-binding-induced change in its distance from a nanoscale quencher bound to the other end of the aptamer.

As an example, there have been studies using colloidal quantum dots to construct detectors of ions. The detection of ions poses a special challenge for nanosensors based on selective binding to analytes; indeed, the most commonly used type of molecules for selective binding are antibodies, which are large proteins that are too large to bind to analytes as small as ions. As has been pointed out, aptamer-based binding is an attractive alternative to antibody-based binding for small analytes.[34,35] As an example of an aptamer-based ion detector, the work Wu et al.[36] is considered; these authors designed a QD-based aptamer beacon for potassium ion detection for potassium concentrations ranging from 0 to 300 mM in water-based solutions. In this work, Wu et al.[36] used CdSe/ZnS quantum dots as the donor and gold nanoparticles as the acceptor in this design; the thrombin-binding aptamer (TBA) was used to bind to the potassium ion. This aptamer has the sequence 5′ GGG TGG TGT GGT TGG 3′. Fluorescence resonance energy transfer (FRET) results in the presence of potassium ions since the aptamer—a tetraplex structure with four GG pairs—undergoes a conformational change that brings the donor and acceptor to within several nanometers of each other. Consequently, the intensity of the quantum dot fluorescence from the solution depends on the percentage of probes that stay in the quenching stage; this intensity, in turn, relates to the potassium ion concentration. In this work, it was observed that the fluorescence intensity of the potassium probe (under laser excitation at 305 nm) decreases with increasing potassium level as illustrated in Fig. 2. Indeed, as illustrated in Fig. 3, the fluorescence response is so significant that it can be seen with the naked eye.

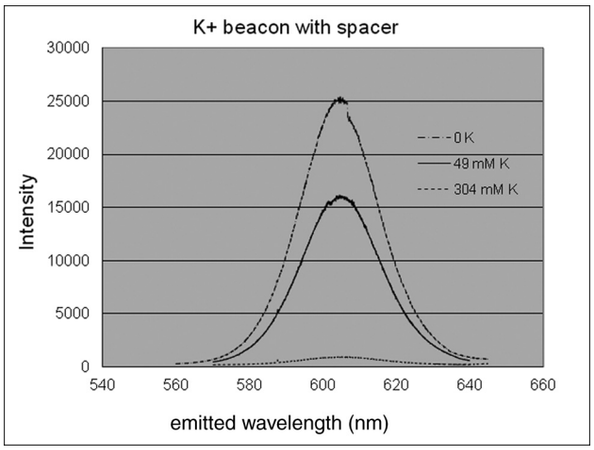

Fig. 2 Fluorescence intensity vs. wavelength for CdSe quantum dots with emission centered at 605 nm; the potassium levels are 0, 49, and 304 mM, as indicated.

Brenneman et al.[37] used semiconductor quantum dots and the same DNA aptamer as Wu et al.[36] for the detection of Hg^{2+} ions. Oligonucleotides can be used for Hg^{2+} ion detection because they interact with thymine (T) bases to create T-Hg^{2+}-T structures (Fig. 4).[38] Q2

Since the TBA (5′-GGT TGG TGT GGT TGG-3′) used for K^+ detection contains six thymine bases, it can also be employed in Hg ion detection. The symmetry of the thymine bases in the TBA will cause the DNA to fold into a hairpin structure when Hg^{2+} binds to it (Fig. 5). When this occurs, the Au nanoparticle, which acts as a quencher through the phenomenon of nanometal surface energy transfer (NSET), is brought closer to the QD. Therefore, this conformational change causes a reduction in the emission of the excited QD. The process of NSET is similar to that of FRET, except the energy transfer is between dipole and surface rather than between dipole and dipole.

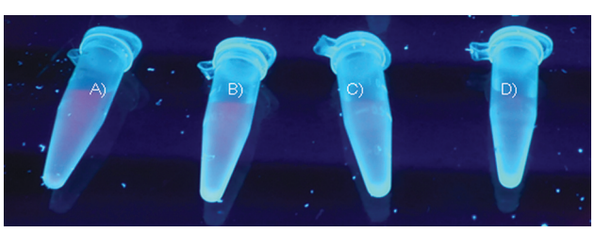

Fig. 3 Each of the four vials—(A), (B), (C), and (D)—contains 1 μL of 907 μM 6-base-spacer beacons. There are 0, 1 μL, 10 μL, 100 μL, 5.69 M saturated potassium chloride added from left to right while all of the volumes are designed to be equal as 1112 μL. This photograph was taken in a dark room with a Panasonic LX3 1 min after potassium ions were added into the beacon solution. The overall potassium ion concentrations are 0 mM (A), 5.11 mM (B), 51.1 mM (C), and 511 mM (D). The overall beacon concentrations of these four vials are the same, 907 μM.

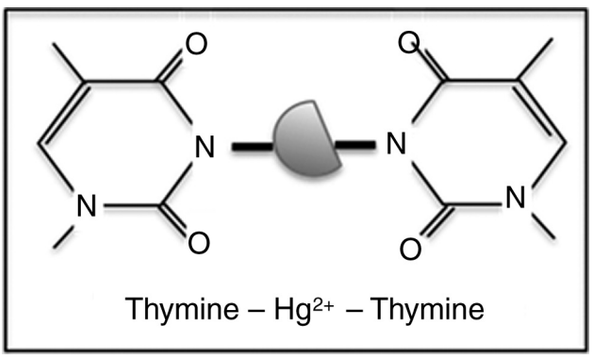

Fig. 4 The interaction between mercury (II) ions and the DNA nucleobase thymine.

This reduction in fluorescence is related to the presence of mercury (II) ions. The emission spectra in Fig. 6 were measured using a spectrometer. Both assays contained 10 nM of the probe, but the addition of 500 nM Hg^{2+} to the probe shows a quenching efficiency of –62%. The quenching efficiency was calculated as $(I_{Hg} - I_0)/I_0$, where I_0 is the peak luminescence intensity of the probe alone and I_{Hg} is the peak intensity of the probe with mercury present.

The decreased peak in Fig. 6 is also blue shifted approximately 13 nm from the control peak. This could be caused by the interaction between a semiconductor and a metal, which can cause band bending. In this assay, there are two possible metals that could cause this: the Au nanoparticles and the mercury (II) ions.

The probe synthesis has several parameters that can be adjusted. The ratio of DNA to QD can be changed to provide a different distribution for the number of DNA strands attached to each QD. While Fig. 5 shows one aptamer attached to the QD for the purpose of illustrating the detection mechanism, the actual probe contains multiple DNA–AuNP conjugates. In Fig. 6, most QDs have around 10 DNA–AuNP conjugates attached. The probe was also synthesized using a ratio of 5:1 and tested at a lower mercury concentration.

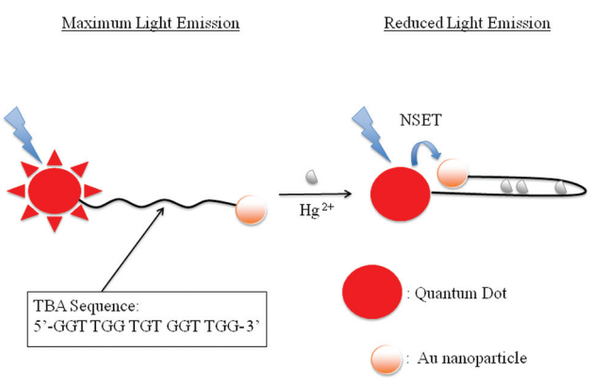

Fig. 5 Schematic of Hg^{2+} ion probe. The interaction between Hg^{2+} and thymine bases leads to the folding of the aptamer, which allows NSET between QD and Au nanoparticle.

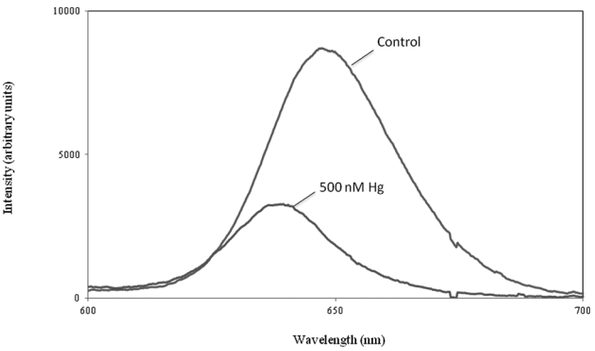

Fig. 6 Photoluminescence of aptamer probe assay at 10 nM probe concentration. Excitation wavelength is 380 nm. Control contains the probe only with maximum emission at 650 nm, and the lower intensity peak is the probe plus 500 nM Hg^{2+} present. Light emission is reduced.

This aptamer-based probe can be used for the optical detection of mercury (II) ions in the nanomolar range. It may be possible to increase the limit of detection using a different probe concentration as well.

The identification of new aptamer-based nanosensors is illustrated by a final example. In Ref. 39, there is an example of an aptamer-based electrochemical biosensing platform for the sensitive detection of the antibody IgE. The base sequence for the aptamer is as follows:

5′-HS-(CH2)6-GCGCG GGGCA CGT*TCA TAACC TTCAG CAAGC TTTAA CTCA***G GGGCA CGTTT ATCCG TCCCT CCTAG TGGCG TGCCC C**GCGC-3′.

Adopting the notation of Ref. 39. the underlined fragments refer to the two complementary arm sequences, the italicized fragment is the random spacer sequence, and the bold fragment is the standard anti-IgE aptamer sequence. This aptamer is known to have its 3′ and 5′ ends in close proximity before the binding to IgE;[40–42] after binding to IgE, the 3′ and 5′ ends are separated by 13.6 nm, which is larger than the FRET radius. Accordingly, this aptamer is Q3

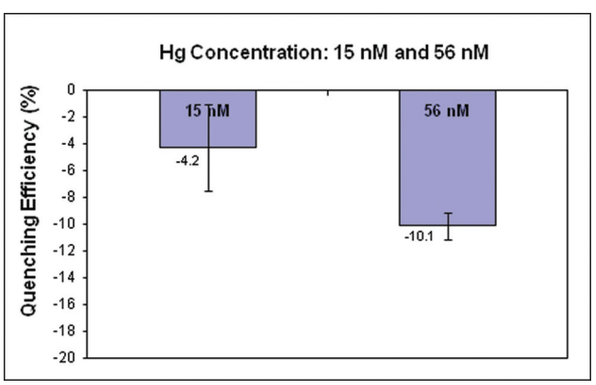

Fig. 7 Quenching efficiency for Hg probe synthesized using a 5:1 DNA-to-QD ratio and then tested at 15 nM Hg and 56 nM Hg.

of the type needed to construct a quantum-dot–aptamer–quencher complex for optical detection of IgE.

CONCLUSION

The foregoing discussions highlight an emerging class of nanosensors based on the use of DNA or RNA molecules that selectively bind to analytes and change their conformational shape. In this article, two separate cases have been highlighted: nanosensors based on 1) nanoscale donor complexes or 2) semiconductor quantum dots. As emphasized in the previous discussions, these novel nanosensors are DNA or RNA molecules that change their conformational state when they bind selectively to an analyte. As discussed previously, the operation of these nanosensors depends on conformational changes that are exploited to produce an electrical signal from a nanoscale donor complex or an optical signature from a semiconductor quantum dot. This class of nanosensors is in a period of rapid growth, and the ultimate detection limit is expected to be that of a single molecule since molecular beacon technology is known to be viable in the single-molecule limit.

REFERENCES

1. Xiao, Y.; Lubin, A.A.; Heeger, A.J.; Plaxco, K.W. Label-free electronic detection of thrombin in blood serum by using an aptamer-based sensor. Angew. Chem. **2005**, *117* (34), 5592–5595.
2. Lai, R.Y.; Plaxco, K.W.; Heeger, A.J. Aptamer-based electrochemical detection of picomolar platelet-derived growth factor directly in blood serum. Anal. Chem. **2006**, *79* (1), 229–233.
3. Xiao, Y.; Qu, X.; Plaxco, K.W.; Heeger, A.J. Label-free electrochemical detection of DNA in blood serum via target-induced resolution of an electrode-bound DNA pseudoknot. J. Am. Chem. Soc. **2007**, *129* (39), 11896–11897.
4. Sun Choi, M.; Yoon, M.; Baeg, J.-O.; Kim, J. Label-free dual assay of DNA sequences and potassium ions using an aptamer probe and a molecular light switch complex. Chem. Commun. **2009**, (47), 7419–7421.
5. Stojanovic, M.N.; de Prada, P.; Landry, D.W. Aptamer-based folding fluorescent sensor for cocaine. J. Am. Chem. Soc. **2001**, *123* (21), 4928–4931.
6. Zuo, X.; Song, S.; Zhang, J.; Pan, D.; Wang, L.; Fan, C. A target-responsive electrochemical aptamer switch (TREAS) for reagentless detection of nanomolar ATP. J. Am. Chem. Soc. **2007**, *129* (5), 1042–1043.
7. Stojanovic, M.N.; Landry, D.W. Aptamer-based colorimetric probe for cocaine. J. Am. Chem. Soc. **2002**, *124* (33), 9678–9679.
8. Tuerk, C.; Gold, L. Systematic evolution of ligands by exponential enrichment: RNA ligands to bacteriophage T4 DNA polymerase. Science **1990**, *249* (4968), 505–510.
9. Liss, M.; Petersen, B.; Wolf, H.; Prohaska, E. An aptamer-based quartz crystal protein biosensor. Anal. Chem. **2002**, *74* (17), 4488–4495.
10. Subramanian, B.; Anne, O.; Steven, S.; David, S. Surface immobilization methods for aptamer diagnostic applications. Anal. Bioanal. Chem. **2008**, *390* (4), 1009–1021.
11. Shlyahovsky, B.; Li, D.; Weizmann, Y.; Nowarski, R.; Kotler, M.; Willner, I. Spotlighting of cocaine by an autonomous aptamer-based machine. J. Am. Chem. Soc. **2007**, *129* (13), 3814–3815.
12. Zhang, J.; Wang, L.; Pan, D.; Song, S.; Boey, F.Y.C.; Zhang, H.; Fan, C. Visual cocaine detection with gold nanoparticles and rationally engineered aptamer structures. Small **2008**, *4* (8), 1196–1200.
13. Baker, B.R.; Lai, R.Y.; Wood, M.S.; Doctor, E.H.; Heeger, A.J.; Plaxco, K.W. An electronic, aptamer-based small-molecule sensor for the rapid, label-free detection of cocaine in adulterated samples and biological fluids. J. Am. Chem. Soc. **2006**, *128* (10), 3138–3139.
14. Zuo, X.; Xiao, Y.; Plaxco, K.W. High specificity, electrochemical sandwich assays on single aptamer sequences and suitable for the direct detection of small-molecule targets in blood and other complex matrices. J. Am. Chem. Soc. **2009**, *131* (20), 6944–6945.
15. So, H.-M.; Won, K.; Kim, Y.H.; Kim, B.-K.; Ryu, B.H.; Na, P.S.; Kim, H.; Lee, J.-O. Single-walled carbon nanotube biosensors using aptamers as molecular recognition elements. J. Am. Chem. Soc. **2005**, *127* (34), 11906–11907.
16. Kim, K.S.; Lee, H.S.; Yang, J.A.; Jo, M.H.; Hahn, S.K. The fabrication, characterization and application of aptamer functionalized Si-nanowire FET biosensors. Nanotechnology **2009**, *20* (23), 235501.
17. Maehashi, K.; Katsura, T.; Kerman, K.; Takamura, Y.; Matsumoto, K.; Tamiya, E. Label-free protein biosensor based on aptamer-modified carbon nanotube field-effect transistors. Anal. Chem. **2006**, *79* (2), 782–787.
18. Robinson, J.T.; Perkins, F.K.; Snow, E.S.; Wei, Z.; Sheehan, P.E. Reduced graphene oxide molecular sensors. Nano Lett. **2008**, *8* (10), 3137–3140.
19. Fowler, J.D.; Allen, M.J.; Tung, V.C.; Yang, Y.; Kaner, R.B.; Weiller, B.H. Practical chemical sensors from chemically derived graphene. ACS Nano **2009**, *3* (2), 301–306.
20. Tung, V.C.; Allen, M.J.; Yang, Y.; Kaner, R.B. High-throughput solution processing of large-scale graphene. Nat. Nanotechnol. **2009**, *4* (1), 25–29.
21. Chen, R.J.; Zhang, Y.; Wang, D.; Dai, H. Noncovalent sidewall functionalization of single-walled carbon nanotubes for protein immobilization. J. Am. Chem. Soc. **2001**, *123* (16), 3838–3839.
22. Debye, P. Dieletric properties of pure liquids. Chem. Rev. **1936**, *19* (3), 171–182.
23. Hummers, W.S.; Offeman, R.E. Preparation of graphitic oxide. J. Am. Chem. Soc. **1958**, *80* (6), 1339–1339.
24. Hernandez, Y.; Nicolosi, V.; Lotya,; Blighe, F.M.; Sun, Z.; De, S.; McGovern, I.T.; Holland, B.; Byrne, M.; Gun'Ko, Y.K.; Boland, J.J.; Niraj, P.; Duesberg, G.; Krishnamurthy, S.; Goodhue, R.; Hutchison, J.; Scardaci, V.; Ferrari, A.C.; Coleman, J.N. High-yield production of graphene by liquid-phase exfoliation of graphite. Nat. Nanotechnol. **2008**, *3* (9), 563–568.
25. Lotya, M.; Hernandez, Y.; King, P.J.; Smith, R.J.; Nicolosi, V.; Karlsson, L.S.; Blighe, F.M.; De, S.; Wang, Z.; McGovern, I.T.; Duesberg, G.S.; Coleman, J.N. Liquid phase production of graphene by exfoliation of graphite in

surfactant/water solutions. J. Am. Chem. Soc. **2009**, *131* (10), 3611–3620.
26. Novoselov, K.S.; Jiang, D.; Schedin, F.; Booth, T.J.; Khotkevich, V.V.; Morozov, S.V.; Geim, A.K. Two-dimensional atomic crystals. Proc. Natl. Acad. Sci. USA **2005**, *102* (30), 10451–10453.
27. Geim, A.K.; Novoselov, K.S. The rise of graphene. Nat. Mater. **2007**, *6* (3), 183–191.
28. Ferrari, A.C.; Meyer, J.C.; Scardaci, V.; Casiraghi, C.; Lazzeri, M.; Mauri, F.; Piscanec, S.; Jiang, D.; Novoselov, K.S.; Roth, S.; Geim, A.K. Raman spectrum of graphene and graphene layers. Phys. Rev. Lett. **2006**, *97* (18), 187401.
29. Graf, D.; Molitor, F.; Ensslin, K.; Stampfer, C.; Jungen, A.; Hierold, C.; Wirtz, L. Spatially resolved Raman spectroscopy of single- and few-layer graphene. Nano Lett. **2007**, *7* (2), 238–242.
30. Gupta, A.; Chen, G.; Joshi, P.; Tadigadapa, S.; Eklund, P.C. Raman scattering from high-frequency phonons in supported n-graphene layer films. Nano Lett. **2006**, *6* (12), 2667–2673.
31. Vasudev, M.; Yamanaka, T.; Jianyong, Y.; Ramadurai, D.; Stroscio, M.A.; Globus, T.; Khromova, T.; Dutta, M. Optoelectronic signatures of biomolecules including hybrid nanostructure–DNA ensembles. IEEE Sens. J. **2008**, *8* (6), 743–749.
32. Puppels, G.J.; Otto, C.; Greve, J.; Robert-Nicoud, M.; Arndt-Jovin, D.J.; Jovin, T.M. Raman microspectroscopic study of low-ph-induced changes in DNA structure of polytene chromosomes. Biochemistry **1994**, *33* (11), 3386–3395.
33. Allen, M.J.; Tung, V.C.; Gomez, L.; Xu, Z.; Chen, L.M.; Nelson, K.S.; Zhou, C.; Kaner, R.B.; Yang, Y. Soft transfer printing of chemically converted graphene. Adv. Mater. **2009**, *21* (20), 2098–2102.
34. Liu, J.; Cao, Z.; Lu, Y. Functional nucleic acid sensors. Chem. Rev. **2009**, *109*, 1948–1998.
35. Keefe, A.D.; Pai, S.; Ellington, A. Aptamer as theraputics. Nat. Rev., Drug Discov. **2010**, *9*, 537–550.
36. Wu, T.C.; Biswas, S.; Dutta, M.; Stroscio, M.A. Quantum dot based aptamer beacon for detection of potassium ions. IEEE Trans. Nanotechnol. *in press*.
37. Brenneman, K.L.; Sen, B.; Stroscio, M.A.; Dutta, M. In *Aptamer-Based Optical Bionanosensor for Mercury(II) Ions*, IEEE Nanotechnology Materials and Devices Conference Proceedings, October 12–15, 2010, Monterey, CA.
38. Ono, A.; Togashi, H. Highly selective oligonucleotide-based sensor for mercury(II) in aqueous solutions. Angew. Chem. Int. Ed. **2004**, *43*, 4300–4302.
39. Wu, Z.-S.; Zheng, F.; Shen, G.-L.; Yu, R.-Q. A hairpin aptamer-based electrochemical biosensing platform for the sensitive detection of proteins. Biomaterials **2009**, *30*, 1950–1955.
40. Gokulrangan, G.; Unruh, J.R.; Holub, D.F.; Ingram, B.; Johnson, C.K.; Wilson, G.S. DNA aptamer-based bioanalysis of IgE by fluorescence anisotropy. Anal. Chem. **2005**, *77*, 1963–1970.
41. Jiang, Y.; Fang, X.; Bai, C. Signaling aptamer/protein binding by a molecular light switch complex. Anal. Chem. **2004**, *76*, 5230–5235.
42. Liss, M.; Petersen, B. Wolf, H.; Prohaska, E. An aptamer-based quartz crystal protein biosensor. Anal. Chem. **2002**, *74*, 4488–4495.

Q1: NMP was defined as *N*-methyl-2-pyrrolidinone. Is this correct?
Q2: Citation of Ref. 67 was changed to that of Ref. 36. Is this correct?
Q3: Is this sentence correct as modified?